Optical and Acoustical Methods in Science and Technology

Bilayer Structures of NiO_x and Pd in Surface Acoustic Wave and Electrical Gas Sensor Systems

W.P. Jakubik*, M. Urbańczyk, E. Maciak and T. Pustelny

Institute of Physics, Silesian University of Technology

Krzywoustego 2, 44-100 Gliwice, Poland

A bilayer sensor structure of nickel oxide NiO_x ($\approx$ 60 nm) with a very thin film of palladium (Pd $\approx$ 18 nm) on the top, has been studied for gas-sensing application at relatively low temperatures of about 30°C and 60°C. The bilayer structure was obtained by rf sputtering and by vacuum deposition (first the NiO_x and then the Pd film) onto a $LiNbO_3$ Y-cut Z-propagating substrate, making use of the surface acoustic wave method, and additionally (in the same technological processes) onto a glass substrate with a planar microelectrode array for simultaneous monitoring of the planar resistance of the layered structure. Such a bilayer structure was investigated in a low concentration range (from 50 ppm to 400 ppm in air) of nitrogen dioxide (NO_2), carbon monoxide (CO) and ammonia (NH_3) in a dry and wet air atmosphere and in a medium hydrogen concentration (1–2.5%) in dry air. The NiO_x and Pd bilayer structure interact rather weakly with NO_2 molecules but with CO and NH_3 this interaction is much greater, especially at higher temperature ($\approx$ 60°C). The hydrogen sensitivity is on the medium level, not exceeding 600 Hz (relative change in the differential frequency of $\approx$ 2.3%) at interaction temperature of 35°C.

PACS numbers: 43.25.Fe, 77.65.Dq, 43.35.Pt, 68.35.Iv, 07.07.Df

1. Introduction

Monitoring the composition of atmospheric gases is the most important requirement for both personal protection and environmental monitoring. The results showing dangerous gas concentrations are usually needed immediately, with a low false-alarm tolerance, high sensitivity and minimum cost. Surface acoustic wave (SAW) gas sensors with a specific layered sensor structure, although clearly not perfect, offer the potential to approach those goals.

SAW gas sensors are very attractive because of their remarkable sensitivity due to changes of the boundary conditions of the propagating wave, introduced by the interaction of an active layered structure with specific gas molecules. This unusual sensitivity results from the simple fact that most of the wave energy is concentrated near the crystal surface within one or several wavelengths. Consequently, the surface wave is in its first approximation highly sensitive to any change of the physical or chemical properties of the thin active sensor structure previously placed on a crystal surface [1, 2]. As long as the thickness of the sensor structure is substantially less than the wavelength of the surface wave, we can speak of a perturbation of the Rayleigh wave (in our case the whole thickness of the layered sensor structure $h \approx 100$ nm and $\lambda = 80$ μm). Otherwise, we have to take into account other types of waves, such as Love waves, which can propagate in layered structures [3].

A very interesting feature of the SAW sensors is the fact that the layered sensor structure (as semiconductor and metal) on a piezoelectric substrate provides new possibilities for detecting gas in a SAW sensor system by using the acoustoelectric coupling between the surface wave and the sensor structure in a high sensitivity interaction region, especially for hydrogen interaction [3–5]. In such a layered sensor structure we can use acoustoelectric interactions in the SAW sensor system as the main detection mechanism. This effect can be many times greater than the commonly used mass effect which is dominant in nonconductive polymer films and simple metal and dielectric films in SAW gas systems [6, 7]. In order to take full advantage of the high sensitivity offered by the SAW sensor through the acoustoelectric effect, the entire conductivity of the sensor structure must be contained in some particular range [8].

The several-layered structures have been examined for this type (metallophthalocyanine + palladium) for the detection of hydrogen [9, 10]. The best are structures with metal-free and copper phthalocyanines and palladium on the top. The structures with metal-free phthalocyanines and palladium display the greatest changes in frequency at various hydrogen concentrations. However, the responses of structures with copper phthalocyanine

* corresponding author; e-mail: wjakubik@polsl.pl

and palladium seem to be faster but display smaller frequency shifts [11].

The idea of bilayer structures in the configuration of semiconductor and palladium on top is very promising and the new structures should be examined. The role of palladium is to increase the whole conductivity of the structure including the important catalytic function. The role of the first semiconductor layer is to shift the palladium metal film from the piezoelectric substrate and also to improve the adsorption properties of the whole structure.

In this paper the new bilayer structures of nickel oxide and palladium are investigated in both SAW and electrical methods towards NO_2, CO, NH_3 and hydrogen concentrations in dry and wet air atmosphere.

2. Experimental setup

Figure 1 shows the idea and photos of the NiO_x + Pd bilayer sensor structure on the piezoelectric and glass substrates in the SAW and electric systems.

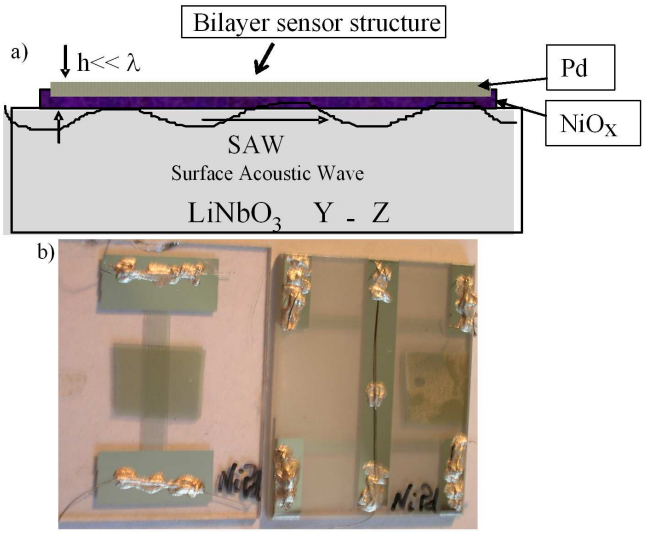

Fig. 1. (a) The bilayer structure of the sensor consists of two layers produced in two different technological processes. The thickness of the sensor material, h, is considerably less than the wavelength, λ, of the SAW; (b) the photos of the investigated layered structure with nickel oxide and palladium thin films — SAW method (right) and electric planar method (left).

On a piezoelectric $LiNbO_3$ substrate (Y cut Z propagation, 20 mm wide, 30 mm long and 2 mm thick) two identical acoustic paths are formed by interdigital transducers. These transducers consist of 20 finger pairs, each 20 μm wide and 20 μm away from the adjacent finger. The operating frequency of each delay line is about 43.6 MHz and the wavelength 80 μm. The interdigital transducers are 14 mm apart from each other. Next, an active sensor structure of NiO_x + Pd is formed in the measuring line by two different technological deposition processes (dc sputtering for NiO_x and vacuum evaporation for Pd thin films).

The whole experimental setup is based on frequency changes in an acoustic surface wave dual delay line system, which is well known [12]. The second path serves as a reference and can compensate for small variations in temperature and pressure. Both delay lines are placed in the feedback loop of oscillator circuits and the response to the particular gas of the active bilayer is detected as a change of the differential frequency Δf, i.e. the difference between the two oscillator frequencies f and f_0. In the electronic circuits we used amplifiers of the type μA 733, and the supplied voltages were usually between 5 and 6 V. Additionally, changes in the electrical resistance of a sample with the same structure made in the same technological process as the SAW device, have been measured. Details concerning this simple electrical planar method are described in literature [13, 14].

The investigated bilayer sensor structure was obtained by means of the two technological methods — first the reactive dc magnetron sputtering process for NiO_x film and then physical vapour deposition for Pd thin film. In both cases a special aluminium foil was prepared for masking of the samples. Before the specific process of the dc sputtering, the piezoelectric and glass substrates were chemically cleaned (in various chemical solvents). The nickel target was used in a controlled atmosphere of $Ar{:}O_2$ (3:1). A uniform film of NiO_x with a thickness of about 60 nm was obtained with quite good adhesion to the substrates of $LiNbO_3$ and glass. A copper–constantan thermocouple was used to control the temperature during measuring tests. The thin (18 nm) palladium layer was formed separately by means of vapour deposition in high vacuum and after the deposition of a NiO_x film in a new process. The thicknesses of the films were monitored by means of the quartz crystal microbalance (QCMB) method with an accuracy of 0.5 nm for Pd and 1 nm for the nickel oxide film. The thickness of the whole sensor structure is considerably smaller than the wavelength of the surface acoustic wave, which is 80 μm. In such a case we can still take into account the disturbation of the Rayleigh surface wave on the piezoelectric substrate [15].

The schematic diagram of the whole experimental setup is shown in Fig. 2. The main part is the measuring chamber, where samples for both SAW and electrical methods are placed. Besides this — the Data Acquisition Switch Unit Agilent 34970A for measuring the temperature and resistance, and Frequency Counter Agilent 53181A for frequency monitoring. The gas flow control system ensures the dosing of the gases to the measuring chamber. The total flow rate of 500 ml/min was used in all measurements, whereas the total volume of the test chamber is about 55 ml. All results are collected in PC through the GPIB interface.

3. Results

The bilayer structure of NiO_x and Pd was investigated towards three different gases such as: NO_2, CO and NH_3

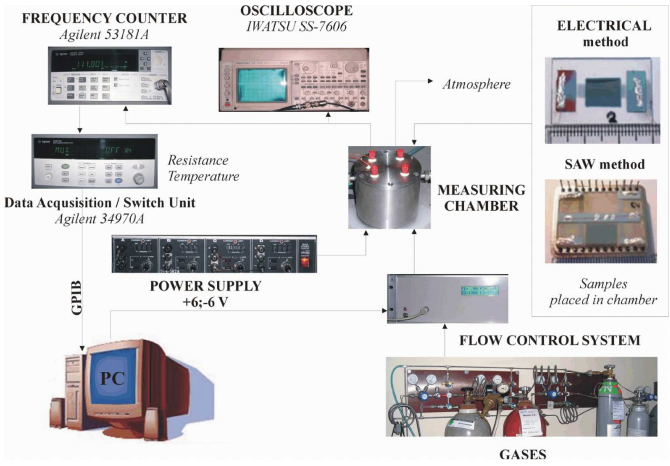

Fig. 2. Schematic diagram of the experimental setup.

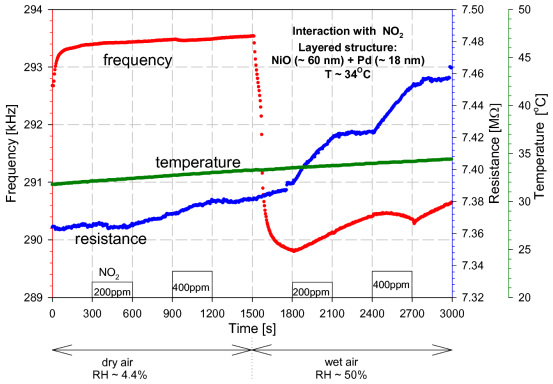

Fig. 3. Interaction of a bilayer structure 60 nm NiO_x + 18 nm Pd, at two various concentrations of NO_2 (200 and 400 ppm) and at a temperature of about 33–35°C in synthetic dry (RH ≈ 4.4%) and wet air (RH ≈ 50%).

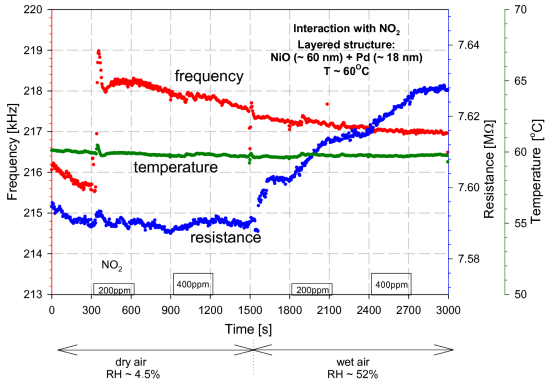

Fig. 4. Interaction of a bilayer structure 60 nm NiO_x + 18 nm Pd, at two various concentrations of NO_2 (200 and 400 ppm) and at temperature of about 60°C in synthetic dry (RH ≈ 4.5%) and wet air (RH ≈ 52%).

in dry and wet air atmosphere and at two interaction temperatures of about 30 and 60°C.

Figure 3 shows an example of the result for the investigated layered structure of NiO_x + Pd, obtained in dry and wet air atmosphere and a cycle of two NO_2 concentrations (200 and 400 ppm) at about 34°C. In the case of these high NO_2 concentrations a very small acoustic interaction is obtained. The differential frequency slightly increases, which is mainly caused by temperature drift. However, a great change in frequency is observed for the air-humidity change. The differential frequency is decreased by about 3.6 kHz when the humidity is changed from 4.4% to 50% r.h. The direction of changes in the frequency signal is connected with the frequency modes configuration. Figure 3 is an example of an inverse frequency mode configuration — the reference line frequency f_0 (≈ 42574 kHz) is smaller than f (≈ 42868 kHz) for the line with the sensor structure. This is an electronic effect; the physical meaning is the amount and direction of frequency changes. In a case like Fig. 3 we have a decrease in the measured frequency under the influence of humidity changes, which is observed as a decrease in differential frequency. Electrical measurements show irreversible increase under NO_2, but only in wet air atmosphere.

At the higher temperature (60°C) the interaction with NO_2 is also very weak, although at the first NO_2 concentration the frequency is increased by above 2 kHz, as in Fig. 4. Similar irreversible increase in resistance is observed for NO_2 dosing but only in wet air, similar as in the lower interaction temperature in Fig. 3.

The interaction with carbon oxide at 35°C is very weak which is shown in Fig. 5. The great change in frequency (increase ≈ 1.8 kHz) and increase in sample resistance (≈ 0.08 MΩ) is observed for the dry to wet air change. The change in frequency interaction (in comparison to Fig. 3) is connected with the frequency modes – this time we have a normal mode configuration. The reference frequency f_0 is greater than the measured frequency. The visible interaction with 100 ppm of CO is observed in wet air atmosphere. The decrease in the absolute value of the sample resistance can be connected with the structural changes under the low temperature (≈ 60°C) annealing.

The acoustic interaction with carbon oxide at 60°C is on the level of 0.7 kHz (for 50 ppm) and 0.5 kHz (for 100 ppm) in a dry air atmosphere, whereas at wet air, this interaction is much greater (even 1.8 kHz) but only for the first CO dosing. The second CO concentration does not cause any frequency shift. This effect is very reversible, even at each measurement cycle which is shown in Fig. 6. For the CO gas a similar decrease in sample resistance (≈ 0.02–0.03 MΩ) is observed in dry and wet air atmosphere. The correlation between acoustic and electrical responses can be related with an acoustoelectric interaction.

In the case of low ammonia concentrations (50 and 100 ppm) the acoustic interaction is on the level of 300 Hz at about 31°C and wet air atmosphere which is shown in Fig. 7. The frequency shift above 400 Hz is also observed when the humidity is changed from a dry to a wet level.

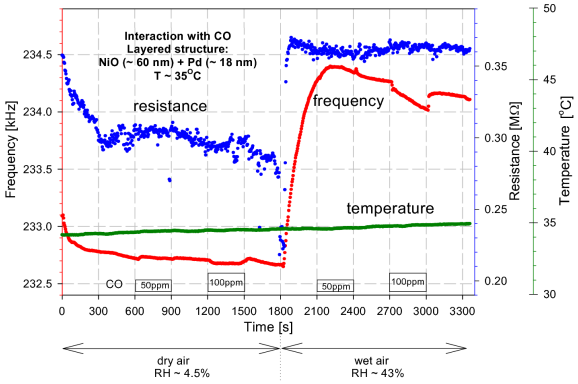

Fig. 5. Interaction of a bilayer structure 60 nm NiO_x + 18 nm Pd, at two various concentrations of CO (50 and 100 ppm) and at a temperature of about 35°C in dry (RH ≈ 4.5%) and wet synthetic air (RH ≈ 43%).

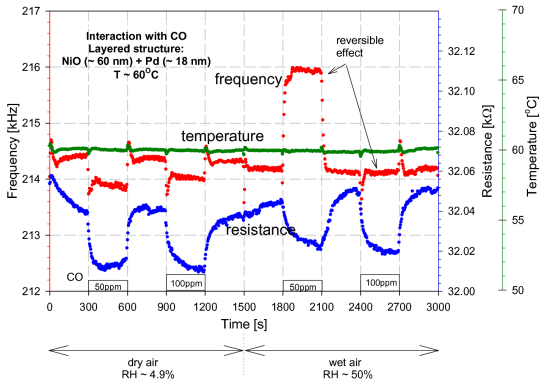

Fig. 6. Interaction of a bilayer structure 60 nm NiO_x + 18 nm Pd, at two various concentrations of CO (50 and 100 ppm) and at a temperature of 60°C in dry (RH ≈ 4.9%) and wet synthetic air (RH ≈ 50%).

The sample resistance does not change under ammonia concentrations, but a very great decrease in resistance (from 5 MΩ to below 0.2 MΩ) is observed for the dry to wet air change.

In the case of higher temperature (60°C) and low ammonia concentrations (50 and 100 ppm) the acoustic interaction is on the level of 200 Hz in dry air atmosphere, which is shown in Fig. 8. The frequency shift is not observed when the humidity is changed from the dry to wet level, but a very great and reversible shift in frequency is observed for the first concentrations of NH_3 in wet air atmosphere.

The sample resistance decreasing on the level of 0.01 MΩ under ammonia concentrations, is similar in both dry and wet air.

The result concerning the same layered structure NiO_x + Pd, obtained in a dry air atmosphere and a cycle of hydrogen concentrations at temperature of about 28°C, is shown in Fig. 9. The differential frequency increases proportionally (almost linearly) to the

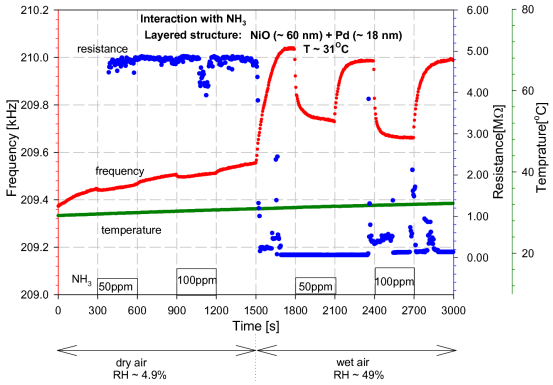

Fig. 7. Interaction of the bilayer structure 60 nm NiO_x + 18 nm Pd, at two various concentrations of NH_3 (50 and 100 ppm) and at a temperature of about 31°C in dry (RH ≈ 4.9%) and wet synthetic air (RH ≈ 49%).

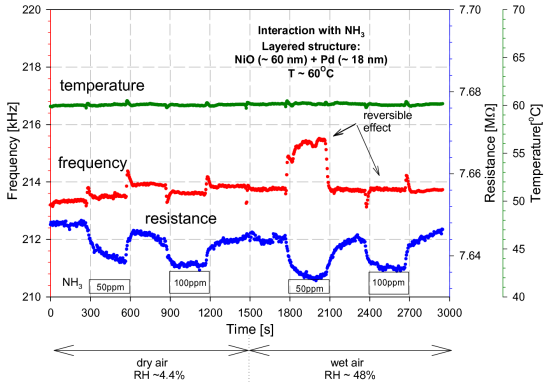

Fig. 8. Interaction of the bilayer structure 60 nm NiO_x + 18 nm Pd, at two various concentrations of NH_3 (50 and 100 ppm) and at the temperature of about 60°C in dry (RH ≈ 4.4%) and wet synthetic air (RH ≈ 48%).

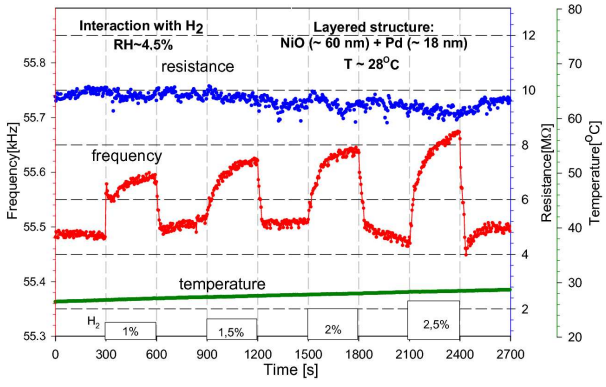

Fig. 9. Interaction in synthetic dry air of a bilayer structure 60 nm NiO_x + 18 nm Pd, at various hydrogen concentrations (from 1% to 2.5%) and at a temperature of about 28°C.

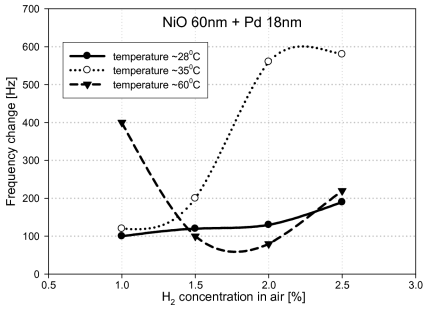

Fig. 10. The change of the differential frequency defined as $\delta(\Delta f) = \Delta f(\text{hydrogen}) - \Delta f(\text{air})$, for the bilayer structure NiO_x 60 nm + Pd 18 nm versus investigated hydrogen concentration in dry air.

hydrogen concentration. The resistance of the sample does not change under hydrogen, and this can be interpreted as a typical mass effect. Figure 10 shows the changes of the differential frequency defined as $\delta(\Delta f) = \Delta f(\text{hydrogen}) - \Delta f(\text{air})$, versus the investigated hydrogen concentration in dry air at three different temperatures.

A great increase of the Δf frequency is obtained at the medium 35°C, which can be interpreted as a change in the crystal phase of PdH_x from α to β [16]. At the higher temperature of 60°C the interaction is lower at the same hydrogen concentrations.

4. Conclusions

A bilayer sensor structure of nickel oxide NiO_x ($\approx$ 60 nm) with a very thin film of palladium (Pd $\approx$ 18 nm) on top, has been studied for gas-sensing application at relatively low temperatures of about 30°C and about 60°C. Such a layered structure was investigated in a low concentration range (from 50 to 400 ppm in air) of nitrogen dioxide (NO_2), carbon monoxide (CO) and ammonia (NH_3) in a dry and wet air atmosphere and in a medium hydrogen concentration (1–2.5%) in dry air.

The interaction of the bilayer structure of NiO_x and Pd with NO_2 gas is rather weak but with CO and NH_3 this interaction is much greater, especially at higher temperature ($\approx$ 60°C). The hydrogen sensitivity is on the medium level, not exceeding 600 Hz (a relative change in a differential frequency of $\approx$ 2.3%) at the interaction temperature of 35°C and dry air atmosphere.

Hydrogen molecules can be detected in the NiO_x + Pd layered structure, but the temperature should be carefully suited to the range of concentrations. At a low temperature of about 28°C the differential frequency increases proportionally (almost linearly) to the hydrogen concentration and the response reaches its steady state quickly. Simultaneously, the response and regeneration times are on the level of several seconds, which is very important from the practical point of view in the detection of highly explosive hydrogen gas.

In all measurements the direction of changes in the differential frequency signal is connected with the frequency mode configuration. In a normal frequency mode configuration — the reference line frequency, f_0, is greater than frequency, f, for the line with the sensor structure. In an inverse mode configuration, the reference frequency, f_0, is smaller than f, in the line with the sensor structure. This is an electronic effect which is connected with the frequency modes in a dual delay line configuration system. The physical meaning is that the amount of frequency changes in a measured line. The resistance decrease of the investigated NiO_x/Pd layered sensor structure can be connected with the structural changes (in the volume or on the surface) under low temperature annealing.

The layered structures with various materials in the SAW sensor system seem to be very promising in gas detection [17–20]. It seems that further research will be focused on the proper fitting of the entire sensor structure to the high sensitivity region for a given piezoelectric substrate, and on the proper construction of the electronic system in order to excite a surface acoustic wave.

Acknowledgments

The work is financed as the grant of Ministry of Science and Higher Education No. RO1 03901.

References

[1] M. Penza, G. Cassano, P. Aversa, A. Cusano, M. Consales, M. Giordano, L. Nicolais, *IEEE Sensors J.* **6**, 867 (2006).

[2] M. Penza, P. Aversa, G. Cassano, W. Wlodarski, K. Kalantar-Zadeh, *Sensors Actuators B* **127**, 168 (2007).

[3] W. Jakubik, M. Urbanczyk, E. Maciak, T. Pustelny, *Bull. Pol. Acad. Sci.* **56**, 133 (2008).

[4] W.P. Jakubik, M. Urbańczyk, S. Kochowski, J. Bodzenta, *Sensors Actuators B* **96**, 321 (2003).

[5] W. Jakubik, M. Urbańczyk, E. Maciak, in: *XX Eurosensors, Goeteborg 2006*, Vol. 1, p. 124.

[6] D'Amico, A. Palma, E. Verona, in: *IEEE Ultrason. Symp.*, Vol. 1, 1982, p. 308.

[7] A. Venema, E. Nieuwkoop, M.J. Vellekoop, W. Ghijsen, A. Barendsz, M.S. Nieuwenhuizen, *IEEE Trans. Ultrasonics Ferroelectrics Freq. Control* **UFFC-34**, 148 (1987).

[8] J.D. Galipeau, L.J. LeGore, K. Snow, J.J. Caron, J.F. Vetelino, J.C. Andle, *Sensors Actuators B* **35-36**, 158 (1996).

[9] W. Jakubik, *Mol. Quantum Acoustics* **25**, 141 (2004).

[10] W. Jakubik, M. Urbańczyk, in: *Proc. IEEE Sensors 2004 Third Int. Conf. on Sensors*, 2004, Vienna University of Technology, 2004, p. 1514.

[11] W. Jakubik, *J. Phys. IV (France)* **137**, 95 (2006).

[12] W. Jakubik, M. Urbańczyk, A. Opilski, *Ultrasonics* **39**, 227 (2001).

[13] O. Varghese, D. Gong, W. Dreschel, K. Ong, C. Grimes, *Sensors Actuators B* **94**, 27 (2003).

[14] H. Wohltjen, W.R. Barger, A. Snow, L. Jarvis, *IEEE Trans. Electron Dev.* **ED-32**, 1170 (1985).

[15] M.J. Vellekoop, *Ultrasonics* **36**, 7 (1998).

[16] M. Tabib-Azar, B. Sutapun, R. Petrick, A. Kazemi, *Sensors Actuators B* **56**, 158 (1999).

[17] T. Pustelny, A. Opilski, B. Pustelny, *Acta Phys. Pol. A* **114**, A-181 (2008).

[18] S. Ippolito, S. Kandasamy, K. Kalantar-Zadeh, A. Trinchi, W. Wlodarski, *Sensor Letters* **1**, 33 (2003).

[19] W. Jakubik, M. Urbanczyk, E. Maciak, T. Pustelny, *Bull. Pol. Acad. Sci.* **56**, 133 (2008).

[20] S. Ippolito, S. Kandasamy, K. Kalantar-Zadeh, W. Wlodarski, *Sensors Actuators B* **108**, 553 (2005).